P2.1   DIRECT OBSERVATION OF THE EVAPORATION OF INTERCEPTED WATER OVER AN OLD-GROWTH FOREST IN THE EASTERN AMAZON REGION

Matthew J. Czikowsky[1]*, David R. Fitzjarrald[1], Osvaldo L. L. Moraes[2], Ricardo K. Sakai[1],
Otávio C. Acevedo[2], Rodrigo da Silva[2], Luiz E. Medeiros[1], and Lucy R. Hutyra[3]

(1) University at Albany, State University of New York, Albany, New York
(2) Universidade Federal de Santa Maria, Santa Maria, RS, Brazil
(3) Harvard University, Cambridge, Massachusetts

1. INTRODUCTION

Interception of rainfall by the forest canopy and the subsequent re-evaporation into the atmosphere constitute an important part of the hydrological balance over forests. Estimates of interception vary from 10 to 30% of annual incident precipitation, depending on forest type, season and precipitation intensity (e.g. Link et al. 2004, Dawson 1998, Helvey and Patric 1965). Furthermore, an appreciable fraction of water vapor in the Amazon is recycled through evapotranspiration and the re-evaporation of intercepted water, with about half of Amazon precipitation being evaporated from the forest (Salati and Vose 1984, Hutyra et al. 2005).

During the process of evaporation of canopy-intercepted water, the leaves are wet, so the stomatal resistance goes to zero. Under such conditions, when surface (physiological) controls are removed, very enhanced rates of evaporation of intercepted water are to be expected from forests compared with shorter vegetation, in all climatic zones (Newson and Calder 1989). While the leaves of the forest canopy are wet, evaporation of intercepted water can proceed at a rate of up to five times the transpiration from surface-dry vegetation (Hewlett 1982). Stewart (1977) found that for a pine forest, only one-third of total evapotranspiration during interception-loss periods was due to transpiration; the other two-thirds was evaporation of intercepted water from the leaf surfaces.

We directly observe the evaporation of intercepted water over an old-growth forest site of the Large-Scale-Biosphere-Atmosphere Experiment in Amazonia (LBA-ECO). We present two case studies where precipitation periods were identified and the latent heat flux was measured by the eddy-covariance method.

---

* *Corresponding author address:* Matthew J. Czikowsky, Atmospheric Sciences Research Center, 251 Fuller Rd., Albany, NY 12203;
e-mail: matt@asrc.cestm.albany.edu

2. LOCATION AND DATA

The data used in this study were collected in an old-growth forest site that was operated as part of LBA-ECO (km67 site). This site is located in the Tapajos National Forest south of Santarém, Brazil, in the eastern Amazon region (Fig. 1).
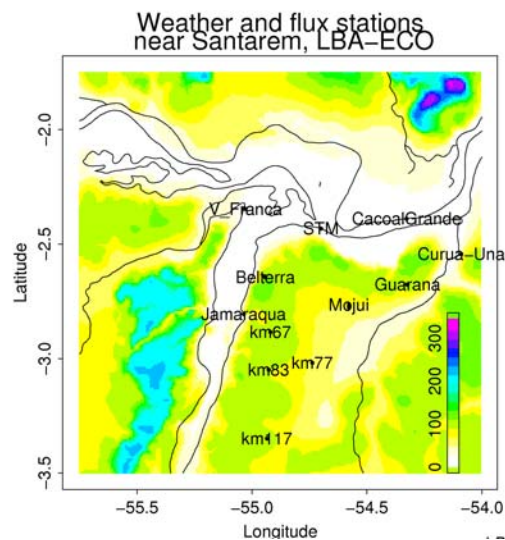

Figure 1: Map of the weather stations and flux-measurement sites operating in the Santarém region (STM) of LBA-ECO. Elevation (m) is shaded. The old-growth forest site where the measurements for the study were taken is denoted as km67 on the map.

An eddy-covariance system that included a Campbell CSAT 3-D sonic anemometer (Campell Scientific, Inc.) and a Licor 6262 CO_2/H_2O analyzer was operating near the top of a 60-m tower at the km67 site. A rain gauge was installed at 42 m height on the tower. A Vaisala CT-25K ceilometer was operating at the site during periods of time from April 2001 to June 2003. The ceilometer provides 15-second measurements of a backscatter profile from the surface to 7500 m at 30-m resolution.

3. METHODS

Precipitation can be detected from the ceilometer backscatter profile, allowing us to identify precipitation periods when the forest canopy intercepted precipitation, including light rainfall events that were not recorded by a rain gauge at the site (Fig. 2). Note that in many cases the precipitation detected in the backscatter profile is measured at the ground (see days 124, 125). However, there are other cases (such as during day 128) when little or no precipitation was measured during periods when precipitation was detected in the backscatter profile, possibly due to factors such as forest canopy interception and wind. Do these light rainfall events provide a large fraction of the re-evaporation?
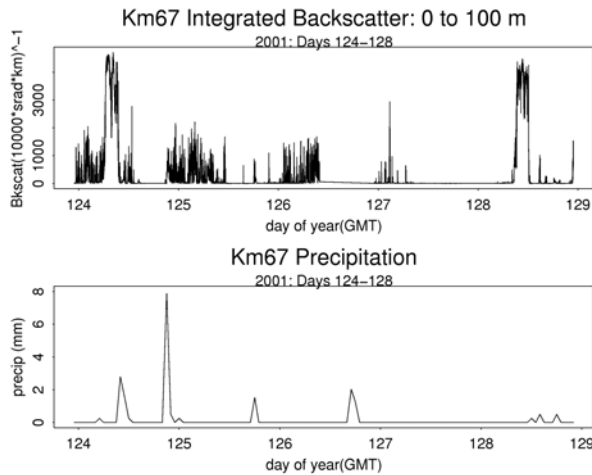

Figure 2: Top panel: Integrated backscatter from 0 to 100 m (units are in 10000*srad*km)$^{-1}$ at the LBA km67 site for May 4-8, 2001 (days 124-128). Bottom panel: Precipitation (mm) measured at km67 during the same time period.

Frequently, sonic anemometers used in the eddy-covariance method fail or operate intermittently during and just after rain. We identify precipitation and interception events from the ceilometer backscatter profile and observe the latent heat flux from the time the eddy-covariance system began functioning during each event until several hours after the end of each event. Latent heat fluxes are calculated every 30 minutes from the eddy covariance system data using the running mean and block-average methods. We present two case studies of precipitation/evaporation events from December 2001.

4. CASE STUDIES

4.1 December 8, 2001 case study

Precipitation fell on this day in the early afternoon during a 15-minute period from 1755 to 1810 GMT (LT + 4 hours) (day of year 341.747 to 341.757), as indicated from the enhanced ceilometer backscatter echoes reported during this time (Fig. 3). The incoming shortwave and photosynthetically active radiation also markedly dropped with the cloudiness associated with the precipitation. No precipitation was measured by the km67 rain gauge for this event. No other rainfall occurred later in the afternoon. The eddy covariance system remained operational during this event, thus allowing for the calculation of latent heat flux.
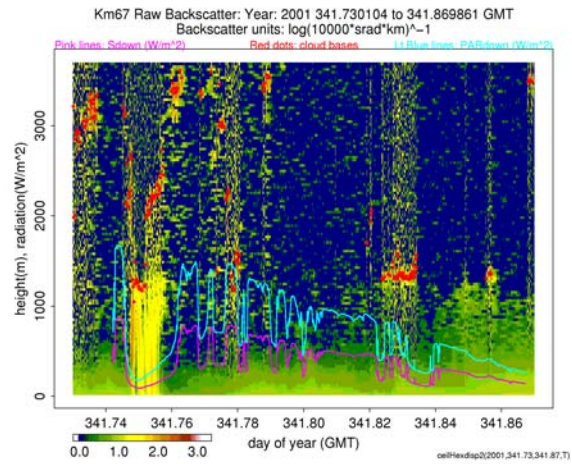

Figure 3: Raw ceilometer backscatter (15-second samples) from 1730 to 2050 GMT on day 341 in 2001 at the LBA km67 site. Backscatter units are log(10000*srad*km)$^{-1}$. Red dots indicate cloud bases (m). The pink line is the incoming shortwave radiation (Sdown, units of W m^{-2}). The light blue line is the incoming photosynthetically active radiation (PARdown, units of W m^{-2}).

Maximum latent heat flux values for the day before the rainfall exceeded 150 W m^{-2}, with a flux of about 130 W m^{-2} just before the rain started (Fig. 4). During the half-hour period that included the precipitation, the latent heat flux as calculated by the running mean method dropped to below 50 W m^{-2}, and then abruptly increased to near 100 W m^{-2} immediately following the event. The block-averaged flux did not show this large increase following the rainfall event. Instead, fluxes dropped followed by a small increase of about 10 W m^{-2} at 1910 GMT (day of year 341.8), one hour

after the end of the rain. Perhaps the 15-minute precipitation event was too short for the block-averaged flux method to capture the flux minimum, with too much of the larger flux surrounding the rainfall period averaged into the result. Fluxes calculated by both methods then decreased with the end of daylight hours approaching.
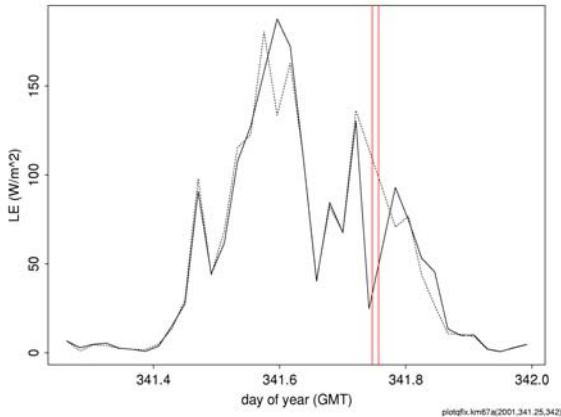

Figure 4: Latent heat flux (W m^{-2}) from 0600 to 2359 GMT on day 341 in 2001 at the LBA km67 site. The black solid line indicates the latent heat flux calculated using a 30-minute running mean. The black dotted line represents the latent heat flux calculated using a 30-minute block average. The left-hand and right-hand side of the pair of red vertical bars indicates the beginning and ending of the rainfall event respectively.

4.2 December 10, 2001 case study

Precipitation fell during two periods on this day. The first event occurred in the early afternoon from 1725 to 1800 GMT (day of year 343.725 to 343.75), as indicated by the enhanced ceilometer backscatter echoes reported during this period (Fig. 5). The rain gauge on the tower at the site recorded 0.762 mm of precipitation during the hour from 1700 to 1800 GMT. A second, lighter rain shower occurred for a brief period in the late afternoon from 2040 to 2055 GMT (day of year 343.86 to 343.87), as shown by the strong ceilometer echoes observed during this time (Fig. 5). No precipitation was recorded by the on-site rain gauge for this second event. The on-site eddy covariance system remained operational during these events; therefore fluxes could be calculated.
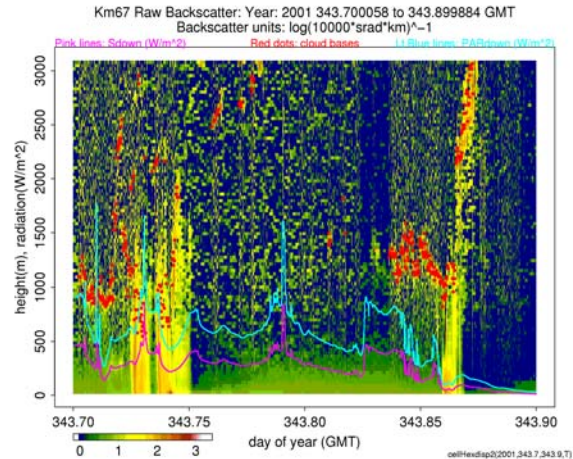

Figure 5: Raw ceilometer backscatter (15-second samples) from 1645 to 2130 GMT on day 341 in 2001 at the LBA km67 site. Backscatter units are log(10000*srad*km)$^{-1}$. Red dots indicate cloud bases (m). The pink line is the incoming shortwave radiation (Sdown, units of W m^{-2}). The light blue line is the incoming photosynthetically active radiation (PARdown, units of W m^{-2}).

Latent heat flux values before the first rainfall of the afternoon exceeded 120 W m^{-2} as calculated by both running mean and block-averaged methods (Fig. 6). There was a sharp decrease in the latent heat flux to below 20 W m^{-2} as calculated by both methods during the first rainfall of the afternoon at 1725 GMT (day of year 343.725). This precipitation event was of longer duration (35 minutes) than the December 8, 2001 case study (15 minutes) and the block-averaged method also captured the flux minimum during rainfall followed by the abrupt flux increase following the rainfall. After the first rainfall and before the second rainfall of the afternoon, the latent heat flux rapidly increased to its maximum value for the day near 140 W m^{-2} around 1910 GMT (day of year 343.8). The latent heat flux as calculated by both methods decreased to below 5 W m^{-2} during the second, late-afternoon rainfall event at 2040 GMT (day of year 343.86). A smaller increase in the latent heat flux of about 20 W m^{-2} was observed at 2135 GMT (day of year 343.9), near the end of the daylight hours as the incoming solar radiation decreased to nighttime values.
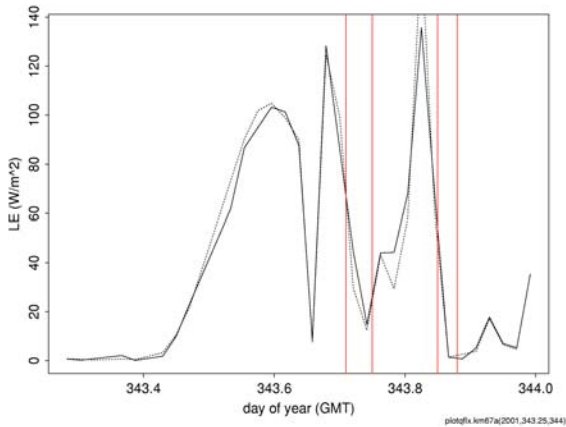
Figure 6: Latent heat flux (W m^{-2}) from 0600 to 2359 GMT on day 343 in 2001 at the LBA km67 site. The black solid line indicates the latent heat flux calculated using a 30-minute running mean. The black dotted line represents the latent heat flux calculated using a 30-minute block average. The left-hand and right-hand sides of the pairs of red vertical bars indicate the beginning and ending of rainfall events respectively.

5. SUMMARY AND FUTURE WORK

We presented two case studies in this abstract. In both cases, large increases in latent heat flux were observed immediately following the precipitation event. Further work will address the factors that account for variations in the magnitude of the observed latent heat flux increases, such as the intensity of the precipitation, time of day of the event, and the degree to which the forest canopy was wetted. Pearce et al. (1980) reported similar daytime and nighttime evaporation rates from a wet forest canopy, and indicated that evaporation from the wet canopy is driven by advected energy not by radiation. Klaassen (2001) stressed the importance of the degree of canopy wetness to estimates of ET from a wet forest canopy.

In continuing work we will analyze many (over 100) of these precipitation events to form an ensemble average from many of these precipitation/interception events. These events presented did capture the re-evaporation following rain, but what about those events when we cannot directly measure fluxes and must fill the data by alternate methods? With large flux increases following precipitation, these time periods cannot be neglected. We plan to compare the observed evaporation for an ensemble of events like the ones presented against the half-hourly evaporation reported using the conventional flux reporting method and also against that predicted by commonly-used models, such as the Penman-Monteith method, and interception model of Gash (1979) to examine the applicability of such methods.

6. ACKNOWLEDGEMENTS

7. REFERENCES

Dawson, T. E., 1998: Fog in the California redwood forest: ecosystem inputs and use by plants. *Oecologia*, **117**, 476-485.

Gash, J. H. C., 1979: An analytical model of rainfall interception by forests. *Quart. J. Roy. Met. Soc.*, **105**, 43-55.

Helvey, J. D., and J. H. Patric, 1965. Canopy and litter interception of rainfall by hardwoods of eastern United States. *Water Resour. Res*, **1**(2), 193-206.

Hewlett, J. D., 1982. Principles of Forest Hydrology. The University of Georgia Press, Athens, GA, 183 p.

Hutyra, L. R., J. W. Munger, C. A. Nobre, S. R. Saleska, S. A. Vieira, and S. C. Wofsy, 2005: Climatic variability and vegetation vulnerability in Amazonia. *Geophys. Res. Lett.*, **32**, L24712, doi:10.1029/2005GL024981.

Klaassen, W., 2001: Evaporation from rain-wetted forest in relation to canopy wetness, canopy cover, and net radiation. *Water. Resour. Res.*, **37**(12), 3227-3236.

Link, T. E., M. Unsworth, and D. Marks, 2004: The dynamics of rainfall interception by a seasonal temperate forest. *Agric. For. Meteor.,* **124**, 171-191.

Newson, M. D., and I. R. Calder, 1989: Forests and water resources: problems of prediction on a regional scale. *Phil. Trans. Roy. Soc. London.* B **324**, 283-298.

Pearce, A. J., L. K. Rowe, and J. B. Stewart, 1980: Nighttime, wet canopy evaporation rates and the water balance of an evergreen mixed

forest. *Water Resour. Res.*, **16**(5), 955-959.

Salati, E., and P. B. Vose, 1984: Amazon Basin: A system in equilibrium. *Science*, **225**, 129-138.

Stewart, J. B., 1977: Evaporation from the wet canopy of a pine forest. *Water Resour. Res.*, **13**, 915-921.